Supplementary Information for

Interpretation of inverted photocurrent transients in organic lead halide perovskite solar cells; proof of the field screening by mobile ions and determination of the space charge layer widths

Rebecca A, Belisle, William H, Nguyen, Andrea R, Bowring, Philip Calado, Xiaoe Li,, Stuart J.C. Irvine, Michael D. McGehee, Piers R.F. Barnes and Brian C. O'Regan

Supplementary Experimental Details.

Some of the mesoporous cells we tested were made with the following variation from the recipe given in the main text. After the deposition of the compact layer, substrates were allowed to cool to room temperature and transferred to a bath of 40 mM $TiCl_4$ (Sigma-Aldrich, 208566) in ultrapure water (Baker, 6906-02) at 70 °C for 30 minutes, rinsed with DI water, and dried for 30 minutes at 70 °C. A 3:7 dilution of 18-NRT TiO_2 paste (Dyesol) in ethanol was spun at 4000 rpm for 30 seconds to form a mesoporous scaffold, and dried for 30 minutes at 120 °C before sintering at 500 °C. Substrates were reheated under hot air and transferred to a dry air box (<5 ppm H_2O) for perovskite deposition. A solution of 1.2 M PbI_2 (Aldrich, 211168) and CH_3NH_3I (Dyesol) in 7:3 γ-BL (Sigma-Aldrich, 90970):DMSO (Sigma-Aldrich, 276855) was prepared in a nitrogen glove box (<5 ppm O_2 and H_2O) and held at 60 °C before deposition. 50 uL of solution was deposited onto substrates and spun at 1000 rpm for 30 seconds and at 5000 rpm for 20 s. 1 mL of toluene (Sigma-Aldrich, 244511) was deposited onto spinning substrates with 10 seconds remaining to remove residual DMSO. Post-spinning, samples were annealed at 100 °C for 15 minutes. Samples were allowed to return to room temperature before spin coating of 75 uL of the hole-transporting material (HTM) solution at 4000 rpm for 30 s. For the HTM, a solution of 72.3 mg of spiro-OMeTAD (Lumtec, LT-S922) and 12 mg spiro-OMeTAD$(TFSI)_2$ in 1 mL of chlorobenzene (Sigma-Aldrich, 284513) was prepared and dissolved at 70 °C for 30 minutes. Spiro-OMeTAD$(TFSI)_2$ was used and prepared as described elsewhere. Once dissolved, the solution was allowed to return to room temperature before the addition of 28.8 uL of tBP and filtering through a 20 nm Al_20_3 filter (Whatman, 6809- 3102) to remove particulate before deposition. After HTM deposition samples were removed from the dry air box and stored in a desiccator at 20% RH before thermal evaporation of 100 nm of Au through a shadow mask to complete the back electrode.

One methylammonium lead bromide cell was also tested that was fabricated by literature methods with some modifications.[1] Briefly, a methylammonium lead bromide solution was prepared by mixing $PbBr_2$ (Sigma-Aldrich) with MABr (Dyesol) in 1:1 molar ratio in a mixture of GBL and DMSO (7:3 v/v) at room temperature for 3 h, and then was filtrated with 0.2 μm syringe filters (PTFE, VWR). The solution was spun coat onto the FTO/c-TiO_2/m-TiO_2 substrates by a consecutive two-step spin coating process at 1,000 and 4,000 r.p.m for 10 and 50 s, respectively. During the second spin-coating step, the substrate was treated with toluene drops. The coated substrates were then dried on a hot plate at 100 °C for 10 min. Spiro and gold were applied following standard procedures.

The CdTe cell shown in figure S6 was fabricated using literature methods with the following modifications.[2] The thickness of the p-type CdTe layer was 3 μm, the thickness of the p+ layer was 330 nm, and silver epoxy (Circuit Works 2400) contacts were applied using a 20 minute 150 °C anneal in air.

(1) N. J. Jeon, J. H. Noh, Y. C. Kim, W. S. Yang, S. Ryu and S. S. Il, *Nat. Mater.*, 2014, **13**, 897.

(2) S.J.C. Irvine, V. Barrioz, D. Lamb, E.W. Jones, and R.L. Rowlands-Jones, *Journal of Crystal Growth*, 2008, 310, 5198

Supplementary Figures

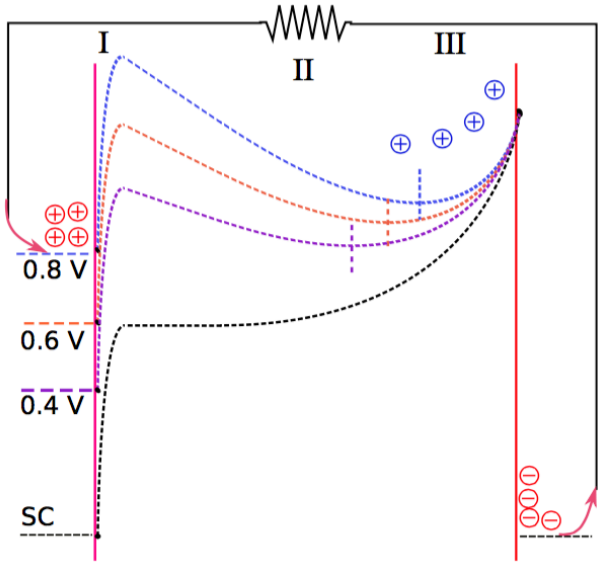

Figure S1. Schematic conduction band energy profiles of a cell with a long screening length on one side. As forward bias potential is applied, the width of region II increases. A light pulse on this cell should therefore give increasingly positive photocurrents with higher voltages, instead of the plateau observed in figure 2. Thus we assert our data is only consistent with cells having screening lengths that are a small fraction of the absorber layer width.

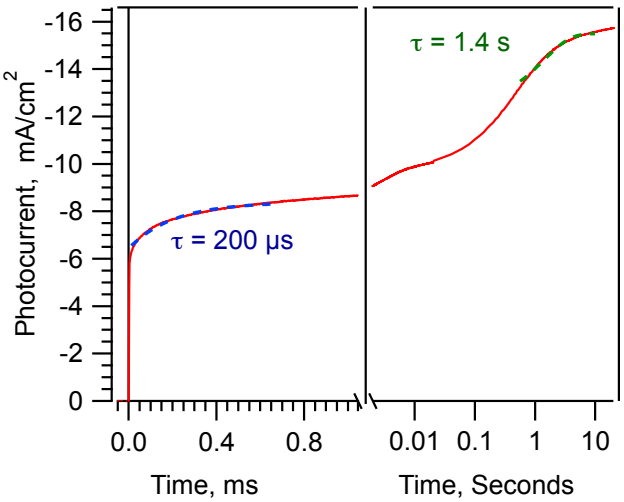

Figure S2. Short circuit photocurrent "turn on" at ~1 sun for a planar TiO_2/MAPI cell. Cell was at dark short circuit for several minutes before the light was turned on at time zero. Note Y scale has been inverted to show "growth" in a normal sense.

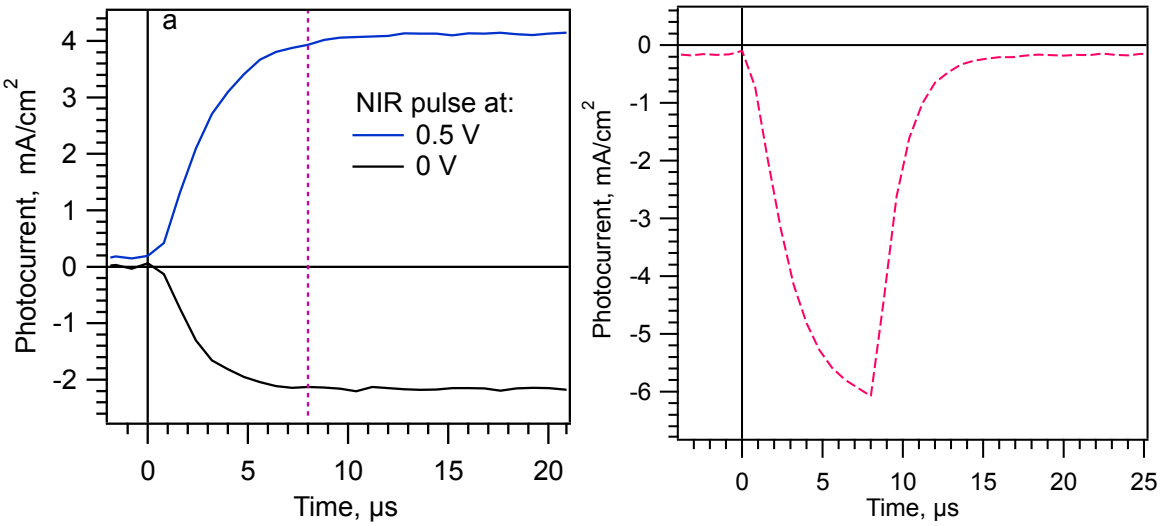

Figure S3. a) Long pulse data for the cell in figure 1b. Dashed vertical line is the end of the 8 μs pulse as used in figure 1. The photocurrent reaches a maximum shortly after 8 μs, with only ~5% additional current. b) Photocurrent transient after holding the cell at 1 V forward bias, dark, for 5 seconds and stepping back to short circuit dark. The pulse was applied 100 μs after the step to short circuit. The time at forward bias near V_{bi} causes the mobile ions to return to a near uniform distribution. Then the step to SC gives an internal potential distribution similar to that in Scheme Ia. This procedure gives the maximum steady state photocurrent, thus we assume it will also give the maximum possible collection of free charges created during the pulse.

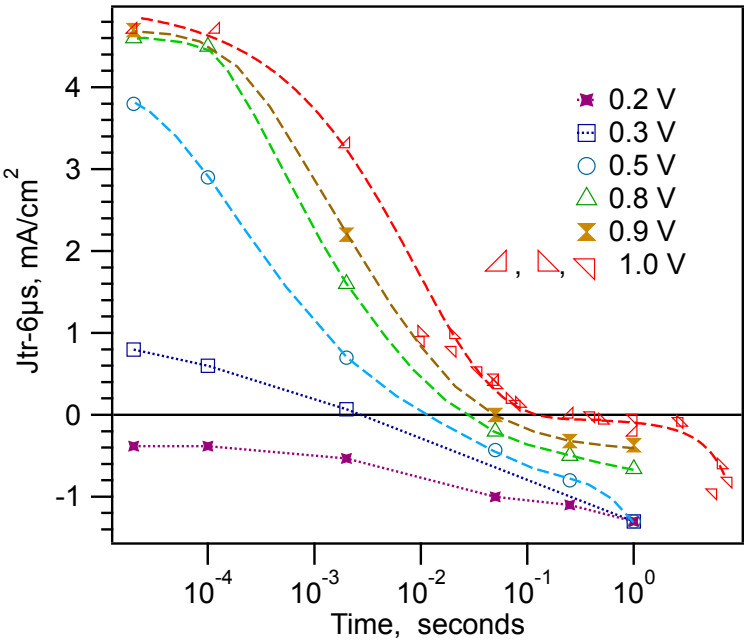

Figure S4. Jtr-6μs with a range applied voltages and dwell times, for a mesoporous TiO_2/MAPI cell that shows the two part evolution. Only at 1 V did we carry the dwell time far enough to see the second part of the evolution. Dashed and dotted lines are guides for the eye.

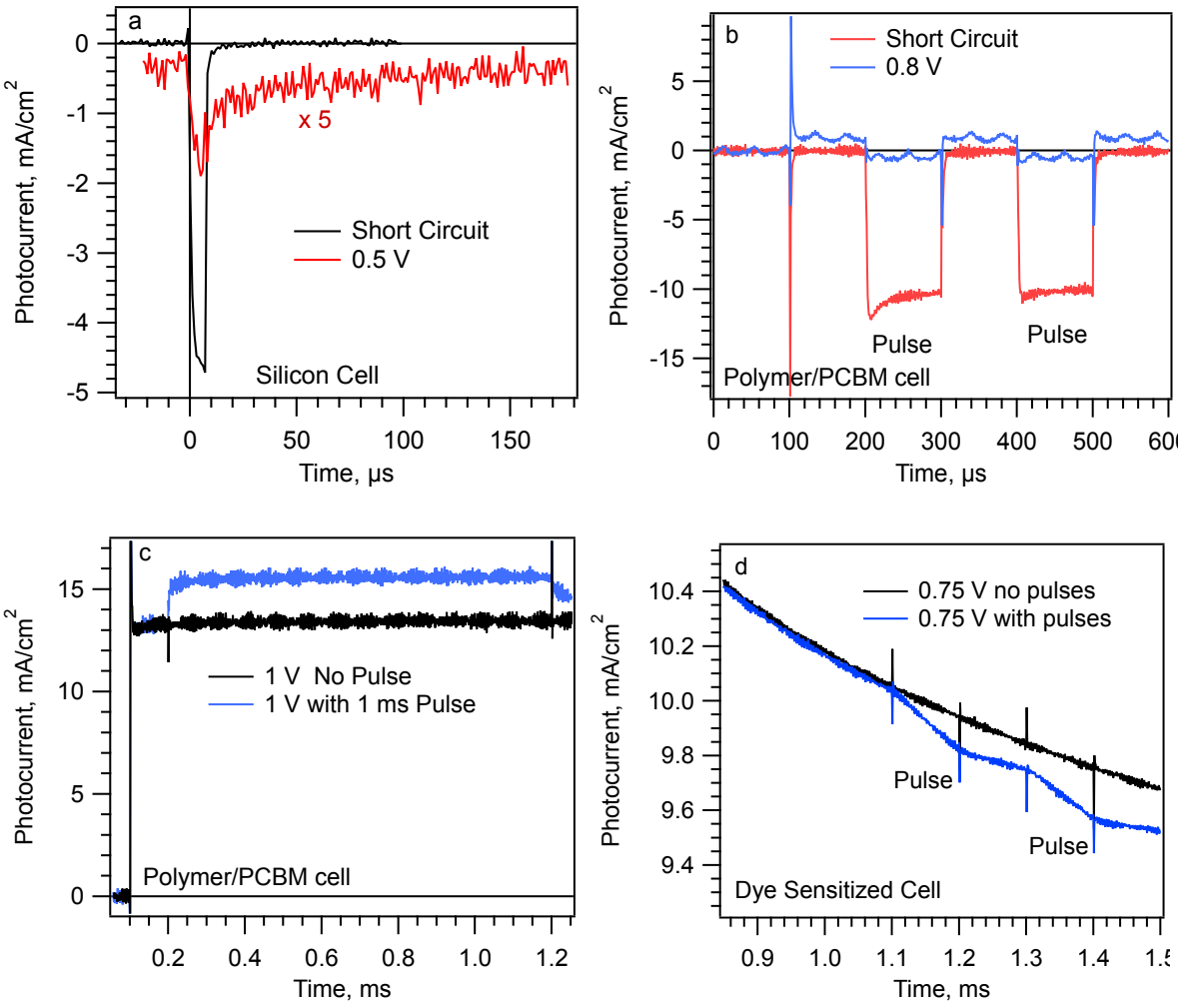

Figure S5. Photocurrent transients (Jtrs) at applied forward bias for other solar cell types. As in the main text, in these figures dark current is positive, short circuit photocurrent is negative. a) Jtrs for a silicon cell for short circuit (SC) and 0.5 V forward bias. Dwell time 20 μs. The transient at 0.5 V is much smaller, but clearly the same sign as the transient at SC. The 1 sun V_{oc} of this particular cell was ~ 0.55 V. b) Jtr at applied forward bias for a polymer/ PCBM cell at 0 V and 0.8 V. The 1 sun Voc for this cell was 0.79 V. Again the transient at 0.8 V is smaller than that at SC, but clearly the same sign. c) A Jtr at 1 V applied bias for the same polymer cell. At this voltage, the transient is positive (in the same direction as the dark current). The 1 ms transient shows no sign of decay, so we conclude this transient is not due to displacement current. Instead, the 1 V bias appears to be beyond the V_{bi}. d) Jtr at 0.75 V on a DSSC. Due to the high capacitance, 100 μs is not enough for the capacitive charging current to dissipate, so the transients are on top of a large positive dark current background. However, it is still clear that the transients are in the negative direction. The 1 sun Voc for this cell was 0.76 V.

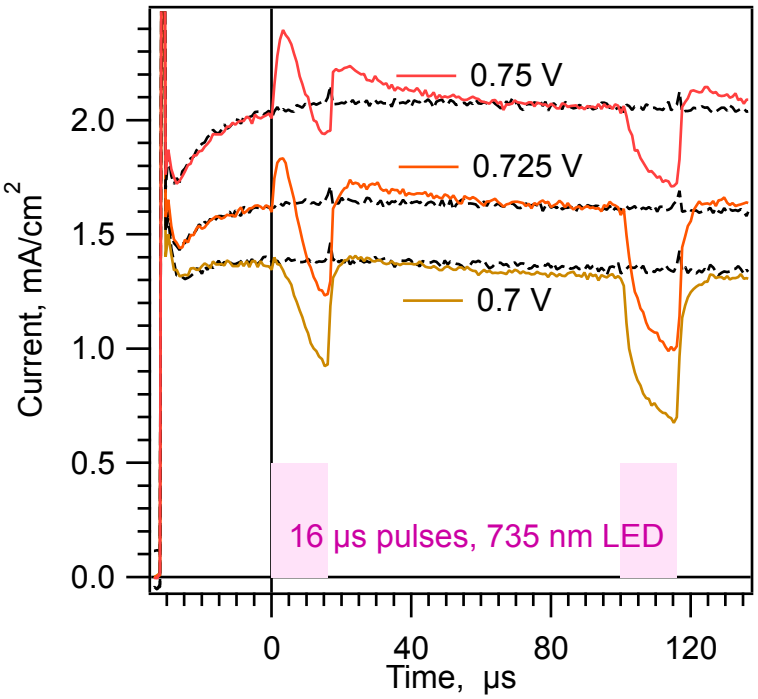

Figure S6. SDP experiments on a CdTe cell. The V_{oc} of this cell was 0.75 V. Black dotted lines are the current for the same applied voltages with the pulse blocked. In this experiment, the CdTe cell does show inverted (positive) transients at high voltage and for very short dwell times. For example, at an applied voltage of 0.75V, with a dwell time of 32 μs, the photocurrent transient is positive for approximately the first 10 μs. With a dwell time of 130 μs at 0.75 V, the transient is already fully negative. There is very little evolution of the Jtr after 130 μs. This contrasts with the MAPI cells where the photocurrent transients at a voltage near V_{oc} require up to 100 ms to evolve from positive to negative, and then continue to evolve for up to 20 seconds. We do not assert that the behavior of the CdTe cell is related to that of the MAPI cell. We include this data for completeness only.

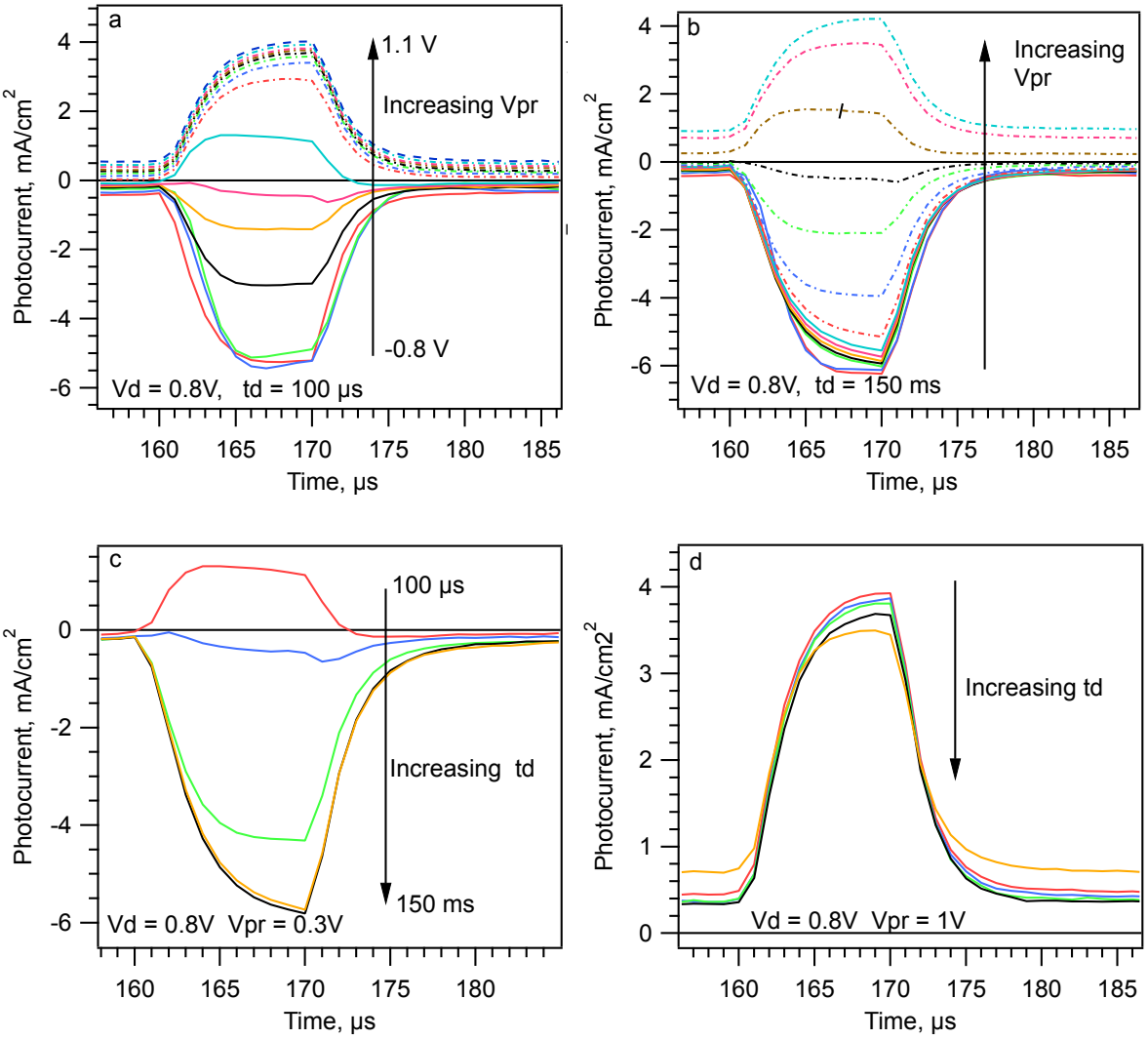

Figure S7. Selected photocurrent transients from SDSP experiments with dwell voltage (V_d) of 0.8 V. a) Dwell time 100 μs; various V_{pr}. b) Dwell time 150 ms; various $V_{pr.}$ c) V_{pr} = 0.3V; t_d from 100 μs to 150 ms. d) V_{pr} = 1 V; t_d from 100 μs to 150 ms

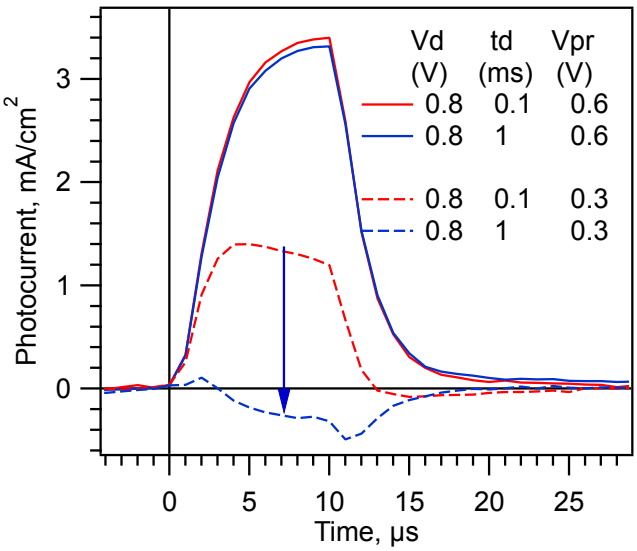

Figure S8. Photocurrent transients from SDSP experiments. Solid lines show that for dwell times of 100 μs and 1 ms at 0.8 V, stepping to a V_{pr} of 0.6 V does not reveal that there has been any change in the band energy profiles. The dashed lines show that for the same dwell voltage and times, a jump to a V_{pr} of 0.3 V will reveal that a change has occurred. The change in Jtr-6μs indicated by the blue arrow on this graph is the same change indicated by the blue arrow in figure 4b.

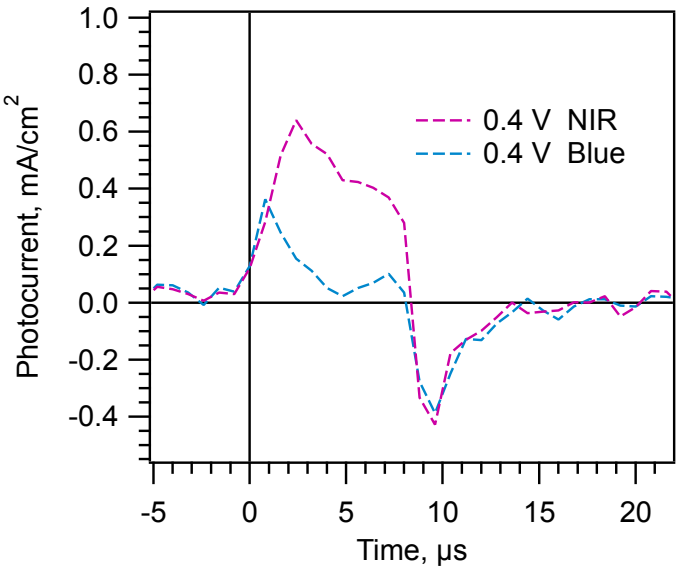

Figure S9. Comparison of the Jtr caused by a blue pulse or NIR pulse with V_d = 0.4 and dwell time 2 ms. The data show that when the blue pulse Jtr is near zero, the NIR pulse Jtr is positive. This is consistent with the NIR pulse being absorbed more strongly in region II, which gives positive photocurrent. Mesoporous TiO_2/MAPI cell.

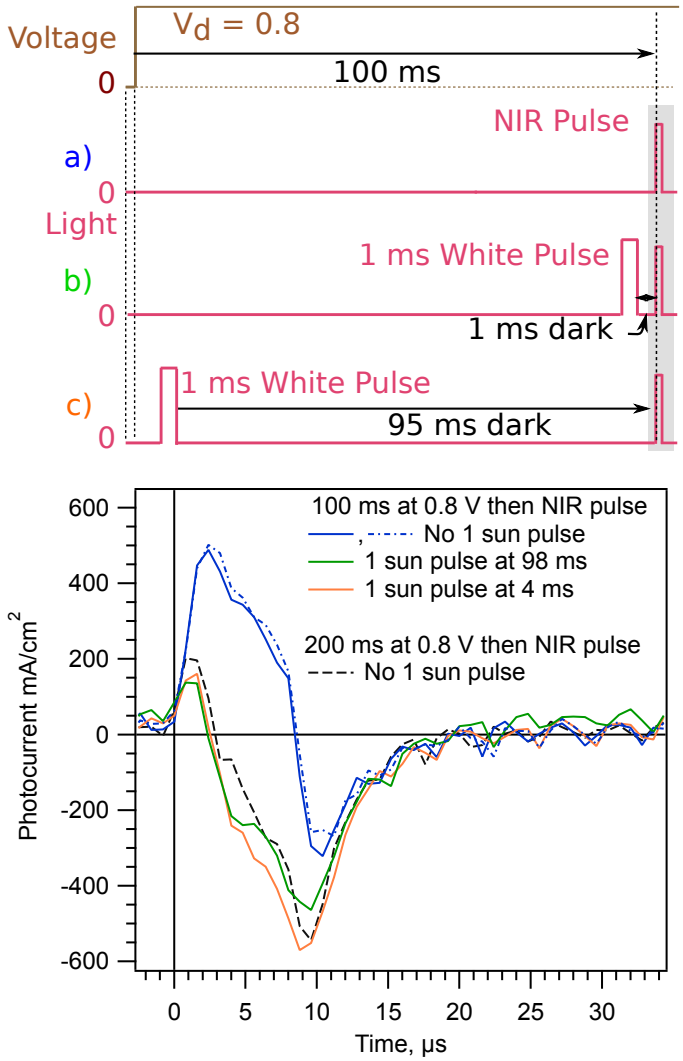

Figure S10. Memory effect of a 1 ms 1 sun pulse at 0.8 V. Top) Schematic of the pulse sequences used for 3 different experiments (a-c). Cell was equilibrated for ≥1 s at SC dark before each experiment. Grey area represents the time period shown in the bottom panel. Bottom) Blue lines are NIR Jtrs measured after 100 ms at 0.8 V in the dark (pulse sequence "a" in top panel).

Orange line is the result from pulse sequence b. A 1 ms 1 sun pulse was added at 98 ms into the 100 ms dwell time at 0.8 V. The preceding 1 sun pulse shifts the following NIR Jtr from positive to negative.

Green line is the result from pulse sequence c. A 1 ms 1 sun pulse was added at 4 ms into the dwell time at 0.8 V. Thus the effect of the 1 ms light pulse decays for 95 ms at 0.8 V dark before the NIR pulse is applied and the Jtr recorded.

Taking into account the noise in the signal, we cannot distinguish the green and orange lines. Thus, there is not more than 10% decay, if any at all, of the "memory" of the 1 sun pulse during 94 ms at 0.8 V dark. A 10% decay in 94 ms would imply a lifetime of about 1 second.

The black dotted line is the NIR Jtr measured after 200 ms at 0.8 V in the dark, showing that, in this case, the effect of the 1 ms 1 sun pulse at 0.8 V is approximately equivalent to an additional 100 ms of 0.8 V in the dark. Cell is a planar MAPI cell.

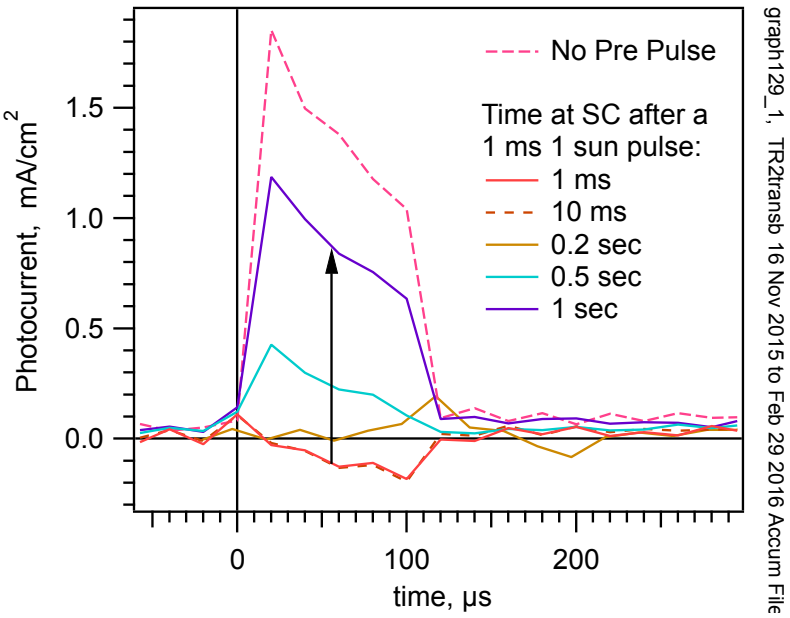

Figure S11. Effect of a 1 ms 1 sun pulse at SC on Jtrs measured after various delay times at SC. Experimental sequence: Equilibrate >1 min at SC dark. Illuminate with 1 ms 1 sun pulse at SC. Delay at SC in dark for times as listed in legend. Switch to 0.8 V dark. Dwell 50 ms. Illuminate with 100 μs NIR pulse and measure Jtr. Dashed line is the Jtr after a 50 ms dwell at 0.8 V with no 1 sun pulse proceeding. This is the baseline condition. Solid red is the Jtr from the above sequence with only 1 ms dark SC delay between the 1 sun pulse and application of 0.8 V bias. The brown dashed line is the Jtr using a 10 ms dark SC delay. As these two are the same, we assert there is no decay of the effect of the light pulse at either 1 or 10 ms. The brown, light blue and purple lines show the decay of the effect of the 1 sun pulse during longer delay times at SC. After 1 sec at SC in the dark, there is still significant "memory" of the proceeding 1 sun pulse.

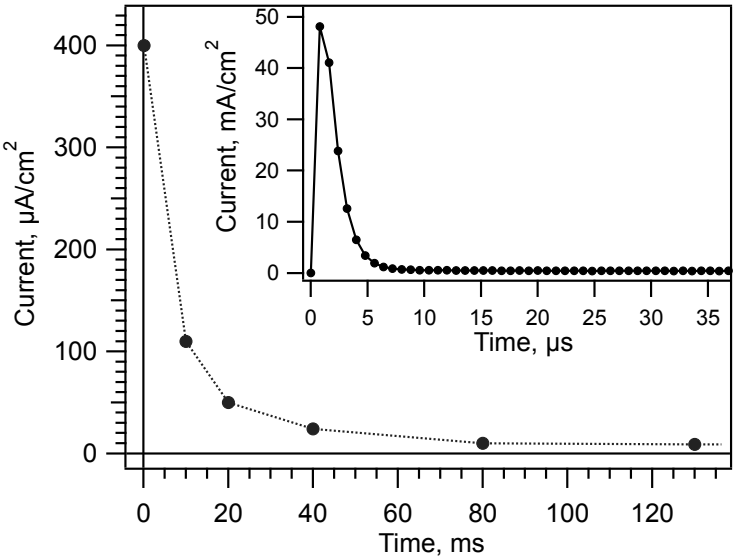

Figure S12. Dark current vs. time at after a step to 0.8 V for a planar MAPI cell. Inset: Dark current vs. time for the first 35 μs after a step to 0.8 V, for the same cell, showing the electrode capacitive charging spike.

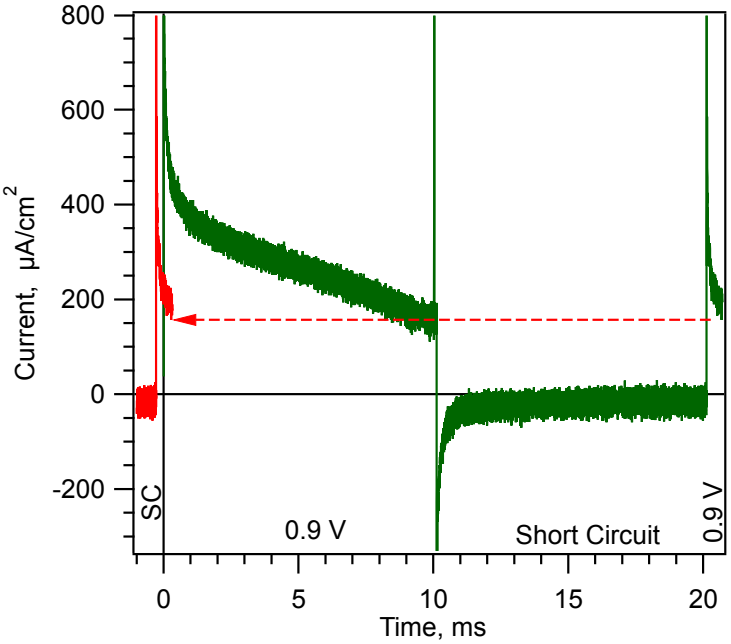

Figure S13. Memory effect of time at forward bias. Cell equilibrated at SC dark for ≥1 minute, then stepped to 0.9 V. Green line shows dark current at 0.9 V. At 10 ms, the cell is switched to short circuit. At 20 ms, the cell is switched back to 0.9 V. The capacitive spike is identical, but by 100 μs the dark current descends to about 1/2 the value of the first 0.9 V period. The red line is the second 0.9 V period shifted back for comparison. Data from a planar cell.

Supplementary Subject I. Are the fast changes in Jtr-6μs shown in figure 3 and 4 (e.g. <5 ms) due to ion movement or dark injected electrons

From the data in figure 4, main text, we find that there is a very fast (≤1 ms) component of the change in the internal potential profile following a change from 0 V to 0.8 V applied bias. This very fast time scale leads us to ask if we are really detecting significant mobile ion movement in 1 ms, or could the fast time scale changes in Jtr-6μs be a result of dark injected electrons and holes flowing into the band valleys and screening the ionic charge. There is a fundamental problem in distinguishing these two effects. At applied bias, as the mobile ions move toward the band valleys the movement of charge internally will result in the measurement of a displacement current in the external circuit. This displacement current will have the same sign as a current resulting from the injection of electronic carriers from the electrodes. Thus, there is no direct way to determine if the dark current we measure externally is the result of charge injection or the motion of mobile ions. We can, however, provide the following likelihood arguments.

To summarize the following discussion, the dark current vs. time behaves as expected for a displacement current, except that the magnitude of the dark current is large enough that it would require a very large ion concentration and/or ion mobility; larger than seems possible. The rest of the discussion below is our attempt to find a solution to this conundrum. We do not give a solid answer. Less than fascinated readers might wish to stop here.

For the cells in this article, the measured dark current, at voltages less than V_{oc}, has most of the characteristics of a displacement current. For example, for a typical planar MAPI cell the dark current decreases strongly with time over the first 100 ms (figure S12). Specifically, at 0.8 V, the dark current first has a capacitive spike, from 0 to ~5 μs. This spike contains around 100 nC/cm^2 of charge; approximately consistent with the flat plate capacitance of the contact electrodes. After the capacitive spike, the dark current decreases steadily to ~10 μA/cm^2 at 100 ms where it stabilizes (figure S12). This 98% decrease with time is the expected pattern for a mainly displacement current, as would be caused by moving ions. If the measured dark current were mainly injected charges from the electrodes, and it was these same charges that filled the band valleys, we might expect the dark current to increase with time. To see this, consider that at V_d = 0.8 V the electrons and holes must overcome injection barriers of ~0.6 V on each side to reach region II (scheme Ic). If the dark injected charges fill the conduction band valleys, the potential distribution will shift towards the situation in Scheme IIIb, solid line. As the voltage drop across region II decreases, the injection barrier for electrons and holes also decreases. This should, all else being equal, increase the injection rate, and thus the dark current should increase with time, rather than decrease as observed.[1]

Another factor is the cells "memory" of previous time at forward bias in the dark (figure S13). For example if we apply 0.9 V for 10 ms, the initial dark current is 600 μA/cm^2 (at 100 μs) and the dark current decreases to 120 μA/cm2 at 10 ms. If we then return to short circuit for 10 ms, and then step back to 0.9 V again, the initial dark current is 280 μA/cm^2 (figure S13). Thus about one half of the effect of the previous period of applied voltage is still present after 10 ms at SC. We note that this memory effect cannot be due to free electrons and holes in the band valleys. Un-trapped electronic charges should flow out of the cell in nanoseconds at SC. The memory effect could be caused by mobile ions that are slow to drift back to their original position after 10 ms at 0.9 V, or to trapped electronic charges. For the memory effect to be due to trapped electronic charges, the timescale requires electron and

hole traps with relatively long detrapping times and also long recombination lifetimes. Moreover, the trapping would have to be inhomogeneous, with more electrons trapped near the Spiro contact and more holes near the FTO contact. (If the trapping were homogeneous, with equal numbers of holes and electrons trapped at each point, the trapped charges would have no effect on the potential profile.) The trapping could have the correct spatial distribution if the trap sites were caused by the presence or absence of the mobile ions in the space charge regions. However, this still requires an unusual type of defect trap that is not a recombination center.

Both the decrease in dark current with time and the memory effect are more easily explained if the initial dark current is mainly a displacement current due to moving ions. However, the magnitude of the dark current then requires a high mobility or high concentration of the ions. We could determine the required values using equation1,

$$J = \mu N_i E, \qquad (1)$$

where E is the electric field across region II after the bias is applied. Unfortunately, estimates of the mobility of the mobile ions cover a wide range [2-7] As an example, we take a mobility of ~1.5 x 10^{-9} $cm^2V^{-1}s^{-1}$ from the middle part of that range.[2,4] At an applied bias of 0.8 V, we estimate region II to be 300 nm wide with a potential drop of ~0.6 V, giving a voltage gradient of 2 x 10^4 V/cm. The dark current at 0.8 V at 100 μs is 450 μA/cm2. From equation 2 we find that this mobility and displacement current would require a mobile ion concentration (N_i) of ~$10^{20}/cm^3$.

This is above the higher end of the estimates of interstitial iodide or iodide vacancies. On the other hand, Yang et.al. have estimated the ion mobility to be ~1 x 10^{-6} $cm^2V^{-1}sec^{-1}$.[5] At this mobility the mobile ion density would have to be ~$10^{17}/cm^3$ to be consistent with the magnitude of the dark current. This density seems reasonable, but the assumed mobility is very high. We conclude that, although it is possible that ≥90% of the measured dark current at times <100 ms could be due to ion drift, it seems unlikely. We note that, if we are indeed observing mobile ions re-equilibrating at the 1- 100 ms timescale, this motion cannot be the same as that responsible for the changes on the 1-10 second timescale. Therefore, we are also forced to conclude there is more than one type of important mobile ion or more than one type of motion.

The high ion mobility or concentration required for the hypothesis that most of the dark current reflects moving ions leads us to propose the following compromise. We propose that most of the observed dark current is electronic, i.e. due to injected electrons and holes, and a smaller fraction is displacement current due to the movement of ions. The data in figure S13 is consistent with this proposal in that the charge extracted at SC, after 10 ms of forward bias, is only 20% of the integrated current during the forward bias period. (Here we are comparing the integrated current up to 10 ms (2.8 $\mu C/cm^2$), which is the injected charged, with the integrated current from 10 to 20 ms (0.6 $\mu C/cm^2$), which is the extracted charge.) This indicates that at least ~80% of the injected charge has transited the cell or recombined in the cell and therefore displacement current due to ion movement is at most 20% of the total current. In this model, the fast effect of bias voltage on the Jtr is caused by the moving ions. To explain the strongly decreasing electronic dark current with time we propose that the movement of the ions also impedes the transit of holes and/or electrons across the cell. That could occur if the movement of the ions increases the blocking efficiency of one or both

electrodes. An improvement in electrode characteristics is consistent with the increase in V_{oc} that is often seen after exposure to forward bias in the dark.

References for Supplementary Subject 1

1 We note that we have reported a different dark current behavior in a previous article. (B. C. O'Regan, P. R. F. Barnes, X. E. Li, C. Law, E. Paomares and J. M. Marin-Beloqui, *J. Am. Chem. Soc*., 2015, **137**, 5087.) In this article, the applied voltage was beyond V_{oc}, and the dark currents were a factor of 10 higher.

2 Y. B. Yuan, J. Chae, Y. C. Shao, Q. Wang, Z. G. Xiao, A. Centrone and J. S. Huang, *Adv. Energy Mater*, 2015, **5**, 1500615.

3 O. Almora, A. Guerrero and G. Garcia-Belmonte, *Appl. Phys. Lett*., 2016, **108**, 043903.

4 D. W. Yang, W. M. Ming, H. L. Shi, L. J. Zhang and M. H. Du, *Chem. Mater.*, 2016, **28**, 4349.

5 T.-Y. Yang, G. Gregori, N. Pellet, M. Grätzel and J. Maier, *Angew. Chem*., 2015, **127**, 8016.

6 P. Delugas, C. Caddeo, A. Filippetti and A. Mattoni, *J. Phys. Chem. Lett*., 2016, **7**, 2356.

7 C. Eames, J. M. Frost, P. R. F. Barnes, B. C. O'Regan, A. Walsh and M. S. Islam, *Nature Comm*., 2015, **6**, 7497.